Molecular dynamics studies of Schottky and Frenkel defects in cerium dioxide

Thabiso Lekoko[1], **Thuto Mosuang**[1], **and Erasmus Rammutla**[1]

[1] Department of Physics & Geology, University of Limpopo, Private Bag x1106, Sovenga, 0727, Polokwane, South Africa

Corresponding author: thuto.mosuang@ul.ac.za

Abstract. Schottky and Frenkel defect energies in cerium dioxide are studied using the classical molecular dynamics. Buckingham potentials are used to understand the cerium-cerium, cerium-oxygen and oxygen-oxygen interactions in the bulk and defect structures. The formulation uses the NVT Evans ensemble to obtain the various defect energies. Oxygen and cerium vacancy defect energies relative to bulk cerium dioxide total energies are used to get more insight on cerium dioxide as a catalyst in exhaust systems. The anion Frenkel-pair defect is the most favourable form of intrinsic ionic defect.

1. Introduction

Cerium dioxide (CeO_2), also referred to as ceria, is the oxide of the rare earth metal cerium. Ceria is an organic solid, mono-constituent appearing under the form of a white ivory to pale beige powder. Generally, it may not be considered as hazardous to human health and the ecosystem environment. This oxide has been under investigation for many applications because of its useful properties [1]-[6]. An exclusive property of ceria is that it has high oxygen mobility, meaning that oxygen atoms within a ceria crystal can diffuse at high rates [1]. Another notable property of ceria is that it can give up some of its oxygen atoms in order to regulate oxygen partial pressures in the atmosphere without actual decomposition [2]. Furthermore, it is utilised as non-reactive base for the burning of nuclear fission products. This means that CeO_2 is remarkably resistant to ion radiations unlike the nuclear fuel, urania (UO_2) because they share the same fluorite crystal structure [3].

CeO_2 of variable composition is generally known as ceria; its unique chemical and electronic properties make it an important material for a number of applications. Easy shifting redox equilibrium in ceria makes it an excellent catalyst for various chemical processes, including production and purification of hydrogen, and carbon monoxide removal from the automobile exhaust. Mobility of oxygen vacancies and consequently high ionic conducting makes ceria a promising electrolyte for solid oxide fuel cells [4] [5]. Electronic structure of ceria leads to its use as UV absorber in cosmetic industry and manufacturing of glass windows [6]. It is also used in light harvesting devices and optical displays [6] [7].

Cerium is mainly used as such in formulation as high precision polishing agent for glass products, as catalyst support for other applications and raw materials for the production of glass and ceramics as well as additions in paints and varnishes [8]. The most important application of CeO_2 is the formation of three way catalysts (TWC) for automobile exhaust gas [7] [8].

Experimental and theoretical studies have shown that transition metal oxides like CeO_2 can be reduced through introduction of defects and/or impurities [9]-[11]. Alternatively, transition metals can be supported on an oxide substrate [12] [13]. Clearly these properties can influence positively the ability of oxides to reduce unwanted gases. It is the objective of this research to introduce Ce and O charged vacancies in the bulk CeO_2 to improve elimination of poisonous gases. This will be accomplished by modelling Schottky and Frenkel related defects type within the fluorite CeO_2 matrix.

2. Computational method

The classical molecular dynamics (MD) calculations using the Daresbury simulation package DL_POLY has been used [14]. In the present study, the Buckingham potentials have been used to accurately reproduce the interactions between the cerium and the oxygen atoms. The ions were allowed to relax using the canonical NVT evans ensemble. The MD used a routine of Verlet leapfrog to integrate the Newton's equations of motion. Simulations were allowed to run with a 10-15 s timestep for a period of 2000 steps and an equilibration after every 200 steps. The ceria supercell is formed of a cube with 4 x 4 x 4 fluorite unit cells, where 256 cerium (Ce) and 512 oxygen (O) atoms are included. Throughout the study, periodic boundary conditions have been functional.

The Buckingham potential [15] is the most common short-range interaction which is given by:

$$V(r_{ij}) = Aexp\left(-{r_{ij}}/{\rho}\right) - \frac{C}{r_{ij}^{6}}, \tag{1}$$

where A, ρ, and C are adjustable parameters, chosen in such a way that they reproduce significant physical properties of real materials. The potential parameters used in this study can be found in a paper by Xu et al. [16]. It must be mentioned that unlike in their potential evaluation, the shell model parameters were excluded in this study, which simply implies that formal charges of -2 for oxygen and +4 for cerium ions are being considered. In order to evaluate the quality of this potential radial distribution functions for a 256 CeO_2 supercell, O vacancy in 256 CeO_2 supercell , and Ce vacancy in 256 CeO_2 supercell are calculated. Oxygen (V_O^{2-}) and Cerium (V_{Ce}^{3+}) vacancies are modelled by the removal of a single atom of each in the 256 CeO_2 fluorite supercell. This results in a defected CeO_2 supercell now having either 511 O atoms or 255 Ce atoms for the V_O^{2-} and V_{Ce}^{3+} vacancy defects respectively. The Schottky defect is modelled by a removal of a Ce atom and two O atoms to depict the removal of a complete CeO_2 formula unit. An in depth assessment of these properties is presented in the subsequent section.

3. Results and discussion

3.1 *Structural properties*

Structural effects due to an O vacancy (V_O^{2-}) and Ce vacancy (V_{Ce}^{3+}) have also been explored at a temperature of 300 K and pressure of 0.0 atm. A radial distribution function **g(r)**, has been used to analyse the consistency of the Buckingham potentials in explaining the interactions within the CeO_2 system. The peak positions in **g(r)** allow a fairly accurate prediction of the most probable distances between the atoms. At equilibrium 300 K, atomic positions for the Ce-Ce, bond lengths peaks appear at 3.8 and 5.4 Å in accordance with the first and second coordination respectively relative to any Ce atom. In the same manner, Ce-O bond lengths peaks appear at 2.3 and 4.5 Å in accordance with the first and second nearest neighbours in reference to a Ce atom, while the O-O peak values appear at 2.8 and 3.8 Å relative to any O reference atom. The **g(r)** of a ceria supercell at 300 K is shown in fig. 1, of which agrees with the simulated annealing of small clusters method of Cordatos et al. [17]. An increase in temperature can also contribute to oxgyen atoms vibrations about their lattice sites. If this vibrational energy exceeds the lattice energy a vacancy get created in the crystal lattice [18]. It can also be seen that creating an O^{2-} vacancy in the material tend to allow Ce atoms to cluster, as their first and second neighbour atoms congregate as displayed in fig. 2. More detailed information on calculated first and second nearest neighbour distances and their respective number of atoms is presented in table 1. Introducing an oxygen vacancy (V_O^{2-}) increases the number of first nearest nieghbors Ce atoms around the Ce atom as the second nearst neighbors are reduced. In contrast, simultaneous introduction of a vacancy and an interstitial oxygen ($V_O^{2\text{-}} - O_{\text{int}}$) in the ceria matrix results in reduction of first and second neighbor O atoms around an O atom. These findings corroborate those reported by Campbell and Peden [19] paper.

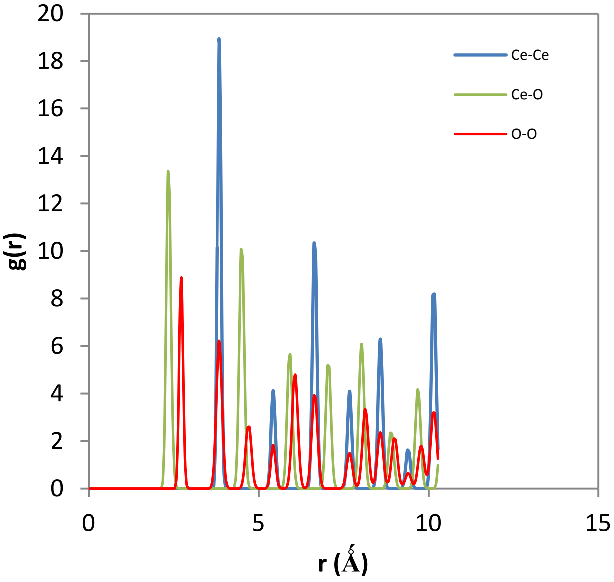

Figure 1. The radial distribution functions of fluorite CeO_2 supercell at 300 K.

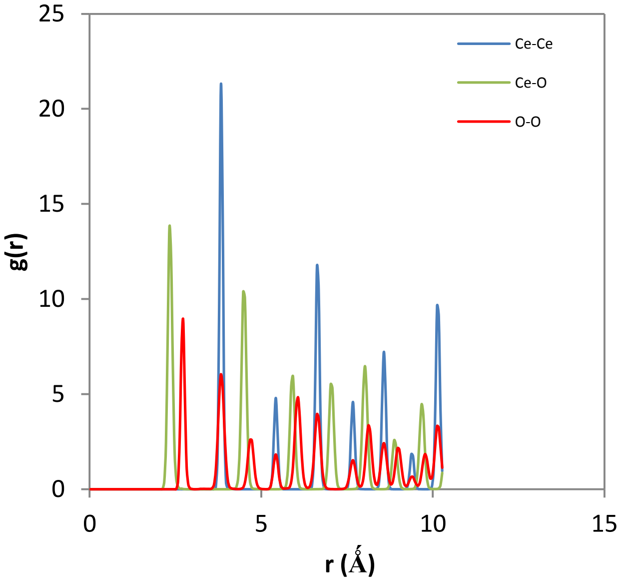

Figure 2. The radial distribution functions of an O vacancy in fluorite CeO_2 supercell at 300 K.

Table 1. Mean first and second nearest neighbour distances (r_1, r_2) and number of atoms (n_1, n_2) in fluorite CeO_2 supercell cell, its O vacancy and an O vacancy-interstitial defect at 300 K.

	Ce-O				Ce-Ce				O-O			
	r_1(Å)	n_1	r_2(Å)	n_2	r_1(Å)	n_1	r_2(Å)	n_2	r_1(Å)	n_1	r_2(Å)	n_2
CeO_2	2.4	2.7	4.5	2.0	3.8	3.8	5.4	2.0	2.8	1.8	3.8	6.0
V_O^{2-}	2.4	2.8	4.5	2.1	3.8	4.3	5.4	1.0	2.8	1.8	3.8	6.0
V_O^{2-}-O_{int}	2.4	2.8	4.6	2.2	3.8	4.5	5.4	1.0	2.8	1.6	3.8	1.2

3.2 *Defect properties*

Investigation of the vacancies, Schottky and Frenkel type defect energies in the fluorite 256 CeO_2 supercell was also performed. The oxygen and cerium vacancies (V_O^{2-} and V_{Ce}^{3+}) in fluorite 256 CeO_2 supercell are created by the removal of either an O^{2-} or Ce^{3+} ions in the supercell. The Schottky defect is obtained by removal of cations and anions in formula units to form vacant lattice sites,

$$\mathrm{Ce_{Ce}} + 2\mathrm{O_O} \rightleftharpoons V_{Ce}^{3+} + V_O^{2-} + \mathrm{CeO_2}(s). \tag{2}$$

From this reaction the Schottky defect energy is calculated using the equation:

$$E_{\mathrm{Schot}}^{\mathrm{CeO_2}} = \frac{1}{3}\left(E[V_{Ce}^{3+}] + 2E[V_O^{2-}] + E[\mathrm{CeO_2}]\right). \tag{3}$$

In a similar manner, a Frenkel defect is created by the displacement of either an anion or a cation to the local interstitial site [20]. Specifically for the favourite oxygen, $O_O \rightleftharpoons O_{\mathrm{int}}^{2+} + V_O^{2-}$. The anion Frenkel-pair defect energy is calculated from:

$$E_{\mathrm{Frenk}}^{\mathrm{ani}} = E[\mathrm{CeO_2}] - E[O_{\mathrm{int}}^{2+} + V_O^{2-}]. \tag{4}$$

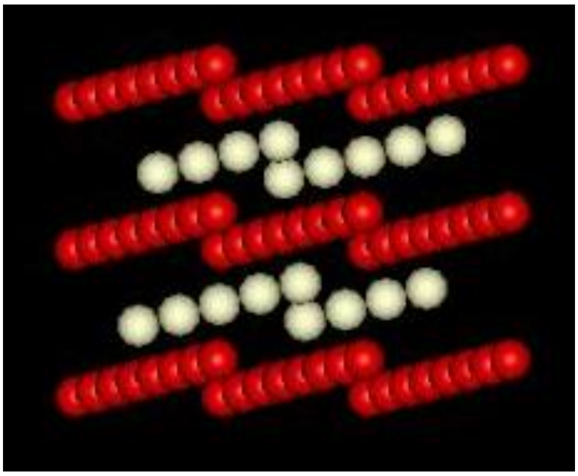

Figure 3. Visualisation of a ceria supercell is organised in a defect free fluorite CeO_2.

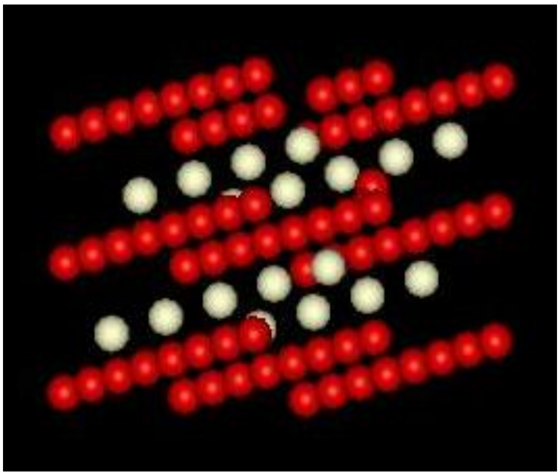

Figure 4. Visualisation of how an O vacancy and O interstitial manifest itself in a fluorite CeO_2 supercell.

Table 1: Defect energies (eV/defect) for all the point, Schottky and Frenkel-pair defects in fluorite CeO_2 using Buckingham potentials in the present work compared with Walsh *et al.* [13].

Defect	Present work	Other calculations
$\boldsymbol{V_O^{2-}}$,	14.66	12.91
$\boldsymbol{V_{Ce}^{3+}}$,	82.74	94.41
Anion Frenkel-pair	-7.37	3.21
Cation Frenkel-pair	2.50	15.94
Schottky defect	2.23	5.79
Defect free	-105.38	-102.87

Two vacancy defects ($V_O^{2-} and\ V_{Ce}^{3+},$), an anion and a cation Frenkel-pair defects, and a Schottky defect have been considered in this investigation. From the present and the Walsh *et al.* [13] calculations, an anion Frenkel-pair defect is the most preferred form of an intrinsic disorder. The anion Frenkel-pair defect according to the present investigation suggest a defect energy of -7.37 eV per defect, whilst the anion Frenkel-pair formation according to Walsh *et al.* [13] suggest a 3.21 eV per defect. The huge deviation on the values (i.e. -7.37 eV/defect and 3.21 eV/defect) could be owed to different procedures of modelling the Frenkel –pair defects. Walsh *et al.* [13] used the intrinsic V_O^{2-} defect energy and the interstitial oxygen (O_{int}) energy defect to calculate the associated anion Frenkel-pair defect energy $(E_{\mathrm{Frenk}}^{\mathrm{ani}})$. This presentation firstly modelled a collective V_O^{2-} and O_{int} defects in one supercell structure, thereafter their mutual defect energy $(E[O_{\mathrm{int}}^{2+}+V_O^{2-}])$ was calculated. This was subtracted from the defect free fluorite 256 CeO_2 lattice energy $(E[\mathrm{CeO_2}])$ as shown in equation (4).

4. Conclusion

The structural and defect conformation properties of ceria have been studied with help of the Buckingham potentials. $\boldsymbol{g}(\mathbf{r})$ and $\boldsymbol{S}(\mathbf{k})$ results demonstrate how the Ce-Ce, Ce-O, and O-O bonds arrange and distribute themselves around a given atom. The nearest neighbour atoms in respect of a given atom can determine the nature of defect in CeO_2. The oxygen vacancy and interstitial defects in the ceria matrix can be explained using the radial distribution functions. Furthermore the calculations show that the anion Frenkel-pair defect has the lowest value as demonstrated by the Walsh *et al.* [13] calculations; suggesting it to occur easily compared to other defect types. This finding promotes the fact that oxygen plays a crucial role in CeO_2 exhaust catalyst.

Acknowledgements

The UL and IBSA are thanked for financial assistance. CHPC is thanked for computational facilities.

References

[1] Gotte A, Hermansson K, Baudin M 2004 *Surface structure* **552** 273.
[2] Zhu WZ, Deevi SC 2003 *Materials science and engineering* A **362** 228.
[3] He H-W, Wu X-Q, Ren W, Shi P, Yao X, Song Z-T 2012 *Ceramics international* **38** S501.
[4] Zhu B, Mat MD 2006 *International Journal of Electrochemical Science* **1** 383.
[5] Gangopadhyay S, Frolov DD, Masunov AE, Seal S 2014 *Journals of alloys and compounds* **584** 199.
[6] Sayle DC, Maicaneanu SA, Watson GW 2002 *Journal of American Chemical Society* **124** 11429.
[7] Gerward L, Staun Olsen J, Petit L, Vaitheeswaran G, Kanchana V, Svane A 2005 *Journal of Alloys and Compounds* **400** 56.
[8] Liu L, Yao Z, Deng Y, Gao F, Liu B, Dong L 2011 *ChemCatChem* **3** 978.
[9] Nakajima A, Yoshihara A, Ishigame M 1994 *Physical Review B* **50** 13297.
[10] Gerward L, Staun Olsen J, Petit L, Vaitheeswaran G, Kanchana V, Svane A 2005 *Journal of Alloys and Compounds* **400** 56.
[11] Chafi Z, Keghouche N, Minot C 2007 *Surface science* **601** 2323.
[12] Sun L-L, Cheng Y, Ji G-F 2010 *Journal of Atomic and Molecular Science* **1** 143.
[13] Walsh A, Woodley SM, Catlow CRA, Sokol AA 2011, *Solid State Ionics*, **184** 52.
[14] Smith W, Forester TR and Todorov IT, 2009 *The DL_POLY 2 User Manual*, STFC Daresbury Laboratory, Darebury, Warrington WA4 4AD Cheshire, UK.
[15] Buckingham RA 1938 *Mathematical and Physical Sciences* **168** 264.
[16] Xu H, Behera RK, Wang Y, Ebrahimi F, Sinnott SB, Wachsman ED, Phillpot SR 2010 *Solid State Ionics* **181** 551.
[17] Cordatos H, Ford D, Gorte RJ 1996 *Journal of Physical Chemistry* **100**18128.
[18] Dutta P, Pal S, Seehra MS, Shi Y, Eyring EM, Ernst RD 2006 *Chemistry of Materials* **18** 5144.
[19] Campbell CT, Peden CHF 2005 *Science* **309** 713.
[20] Guglielmetti A, Chartier, van Brutzel L, Crocombette J-P, Yasuda K, Meis C, Matsumura S 2008 *Nuclear Intsruments and Methods in Physics Research* B **266** 5120.